

## Article

# Monthly Variation and Ultraviolet Stability of Mycosporine-like Amino Acids from Red Alga Dulse *Palmaria palmata* in Japan

Yuki Nishida <sup>1</sup>, Yoshikatsu Miyabe <sup>1,2</sup>, Hideki Kishimura <sup>3</sup>  and Yuya Kumagai <sup>3,\*</sup> 

<sup>1</sup> Marine Chemical Resource Development, Graduate School of Fisheries Sciences, Hokkaido University, Hakodate 041-8611, Hokkaido, Japan; karakuchi@eis.hokudai.ac.jp (Y.N.); yoshikatsu\_miyabe@aomori-itc.or.jp (Y.M.)

<sup>2</sup> Food Research Institute, Aomori Prefectural Industrial Technology Research Center, 2-10 Chikkogai, Hachinohe-shi 031-0831, Aomori-ken, Japan

<sup>3</sup> Marine Chemical Resource Development, Faculty of Fisheries Sciences, Hokkaido University, Hakodate 041-8611, Hokkaido, Japan; i-dulse@fish.hokudai.ac.jp

\* Correspondence: yuyakumagai@fish.hokudai.ac.jp; Tel.: +81-138-40-5560

**Abstract:** Mycosporine-like amino acids (MAAs) are the natural ultraviolet (UV)-absorbing compounds from micro- and macro-algae. The MAAs in algae change with the environmental conditions and seasons. We previously determined an efficient extraction method of MAAs from red alga dulse in Usujiri (Hokkaido, Japan) and revealed monthly variation of MAA in 2019. Dulse samples in 2019 for MAA preparation were suitable from late February to April. In this study, to confirm the suitable timings to extract MAAs from Usujiri dulse, we also investigated the monthly (from January to May) variation of MAA content in 2020. There were the most MAAs in the sample on 18 March (6.696  $\mu\text{mol g}^{-1}$  dry weight) among the samples from January to May 2020. From two years of investigation, we deduce that samples of Usujiri dulse from late February to early April were suitable for MAA preparation. The UV stability of the two major purified MAAs in Usujiri dulse—palythine and porphyra-334—was tested. The two MAAs and 2-hydroxy-4-methoxybenzophenone were stable for up to 12 h under a 312 nm lamp at 200  $\mu\text{W cm}^{-2}$ , but 2-ethylhexyl-4-methoxycinnamate formed a cis/trans-mixture in a short time. The data in this study show the suitable sampling period for Usujiri dulse and the possible application for UV protection from food and cosmetics.

**Keywords:** red alga; dulse; mycosporine-like amino acids; monthly variation; ultraviolet stability; ultraviolet absorption; Usujiri Hokkaido



**Citation:** Nishida, Y.; Miyabe, Y.; Kishimura, H.; Kumagai, Y. Monthly Variation and Ultraviolet Stability of Mycosporine-like Amino Acids from Red Alga Dulse *Palmaria palmata* in Japan. *Phycology* **2021**, *1*, 119–128. <https://doi.org/10.3390/phycolgy1020009>

Academic Editor: Peer Schenk

Received: 31 October 2021

Accepted: 22 November 2021

Published: 25 November 2021

**Publisher's Note:** MDPI stays neutral with regard to jurisdictional claims in published maps and institutional affiliations.



**Copyright:** © 2021 by the authors. Licensee MDPI, Basel, Switzerland. This article is an open access article distributed under the terms and conditions of the Creative Commons Attribution (CC BY) license (<https://creativecommons.org/licenses/by/4.0/>).

## 1. Introduction

Although sunlight is essential for photosynthesis in plants, it also contains harmful ultraviolet (UV) for organisms. UV radiation is classified into UVA (315–400 nm), UVB (280–315 nm), and UVC (200–280 nm) in terms of their spectra. UVC does not reach Earth since it is absorbed in the ozone layer. UVA and UVB cause defects of metabolic function, oxidation of DNA and RNA, and production of reactive oxygen species (ROS) [1,2]. While UV has beneficial effects for humans, such as the innate immunity response and biosynthesis of vitamin D [3], it also induces skin disorders in humans, e.g., erythema, pigmentation, edema, formation of sunburn, phototoxicity, and photoaging [4–7]. Therefore, UV protection agents such as UV absorption agents and UV scattering agents are used for the protection of our skin. However, the use of these agents has raised safety concerns for the human body and environment. Some agents may cause oxygen radical production, cancer, and photoallergic skin inflammation [8–10], while some cause coral bleaching even in low concentrations [11]. Alternative compounds such as polyphenols and flavonoids from natural products have been used as UV protection agents [12–14], and natural UV protection products with a high molar extinction coefficient are now in demand.

Red alga dulse (*Palmaria palmata* in Japan), which is distributed in the Northern Iwate prefecture and northward, is an underused marine resource. Dulse has been removed from Kombu rope in Hakodate, Hokkaido, since Kombu is an important resource for the local fishermen. When dulse is utilized as a novel local food, we have studied its components and functions for human health, such as antioxidant activity, peptides for the inhibition of angiotensin I-converting enzyme activity, prebiotics from xylooligosaccharides [15–18], and its mitochondrial and chloroplast genome and phycobiliprotein structures [19–21]. In addition, dulse contains UV absorption compounds such as mycosporine like amino acids (MAAs) [22]. MAAs, secondary metabolites of nitrogen products with cyclohexanone or cyclohexenimine structures, are water soluble low-molecular compounds synthesized by the shikimate and pentose phosphate pathways [23,24]. MAAs are used as UV protection compounds in marine organisms [25–27]. More than 30 MAA structures with absorption spectra from 310 to 360 nm have been reported to have a high molar extinction coefficient ( $\epsilon = 28,000\text{--}50,000$ ) [28–30]. MAAs release heat from UV radiation instead of producing ROS [31–33]. However, a problem with utilizing MAAs for UV protection materials is their low content in seaweeds. The maximum MAA content to have been reported is 14 mg/1 g dry weight [34,35]. Therefore, we investigated an effective MAA extraction method using underused Usujiri dulse [22], involving six hours of water extraction to form dulse powder. We found that dulse from 25 February 2019 contained a high quantity of MAAs when compared with samples from earlier (to January) and later (to May) in 2019.

In this study, we investigated the monthly variation of MAAs in Usujiri, Hokkaido, from January to May 2020 to clarify the suitable dulse sampling periods. To demonstrate the suitable application of MAAs as UV protection materials, we evaluated the UV stability of two purified MAAs, palythine and porphyra-334, in strong UV conditions.

## 2. Materials and Methods

### 2.1. Algal Samples

All dulse samples were collected at 1 m depth in Usujiri, Hakodate, Japan, from January to May 2020. After collection, the thalli were washed with tap-water to remove sea salt and epibionts. Soon after, they were frozen and lyophilized. Dried algal samples were ground into a fine powder by a Wonder Blender WB-1 (Osaka Chemical Co., Osaka, Japan) and stored in the dark at room temperature until analysis.

### 2.2. Extraction of Crude MAAs from Dulse

The optimum extraction condition of MAAs from dulse was determined in a previous study [22]. Accordingly, the fine powder samples were soaked in 20 volumes ( $v/w$ ) of distilled water at 4 °C for 6 h, and the water extracts were collected by centrifugation at 4 °C,  $27,200\times g$ , for 10 min. After centrifugation, supernatants were lyophilized and soaked in 20 volumes (volume/powdered sample weight) of methanol at 4 °C for 2 h. The methanol extracts containing MAAs were centrifuged at 4 °C,  $27,200\times g$ , for 15 min. The supernatants were evaporated, re-dissolved in water, and lyophilized. Then, the solid samples were designated as crude MAAs and used in the following experiments.

### 2.3. Spectrophotometric Analysis of MAAs

Crude MAAs solutions were analyzed by the UV-visible ray absorption spectrum using a spectrophotometer (UV-1800, Shimadzu, Kyoto, Japan).

### 2.4. Separation of MAAs by High Performance Liquid Chromatography (HPLC)

The crude MAAs were dissolved in water containing 0.1% trifluoroacetic acid (TFA) and the solution underwent sequential filtration by a Millex-GV (diameter: 25  $\Phi$ mm, pore size: 0.22  $\mu$ m) (Merck Millipore, Billerica, MA, USA) and Millex-LG (diameter: 4  $\Phi$ mm, pore size: 0.20  $\mu$ m) (Merck Millipore, Burlington, MA, USA). The filtrated MAAs were isolated by reversed-phase HPLC with a Mightysil RP-18GP column (5  $\mu$ m, 10  $\times$  250 mm) (Kanto Kagaku, Tokyo, Japan) using isocratic elution of ultra-pure water containing 0.1%

TFA for 7 min and a linear gradient of acetonitrile (0–70%) containing 0.1% TFA for 13 min at a flow rate of 4.73 mL/min. The column oven temperature was set at 40 °C. The detection wavelength was set at 330 nm. The peaks of 330 nm were fractionated and evaporated. Then, the purified MAAs were dissolved in an appropriate quantity of distilled water.

### 2.5. Ultraviolet Stability

Palythine and porphyra-334 were prepared by HPLC from dulce powder on 25 February 2019. The purified palythine and porphyra-334 were dissolved in 0.1 M sodium phosphate buffer (pH 7.4) at a concentration of  $2.2 \times 10^{-5}$  M. Then, 2-Hydroxy-4-methoxybenzophenone and 2-ethylhexyl-4-methoxycinnamate (Tokyo Kasei Kogyo, Tokyo, Japan) were used as positive and negative standards, respectively. UV-B radiation (312 nm) was generated by CSF-15BF (Cosmo Bio Co., Ltd., Tokyo, Japan), and the strength of radiation at  $200 \mu\text{W}/\text{cm}^2$  was set by the distance from the UV-B generator. After UV-B exposure, the spectra were measured for up to 12 h by a spectrophotometer.

### 2.6. Phycoerythrin (PE) Content

The PE of each sample was prepared from fine powders. Namely, 10 mg of each powder was dissolved in 1 mL distilled water and extracted at 4 °C for 12 h. After centrifugation at  $12,000 \times g$  for 5 min, the spectra of supernatants were measured. The quantity of PE was determined by the following equation:  $\text{PE (mg/mL)} = [(A_{564} - A_{592}) - (A_{455} - A_{592}) \times 0.2] \times 0.12$  [35].

### 2.7. Abiotic Data in Hakodate

The monthly mean daily maximum ultraviolet index (UVI) was obtained from the Japan Meteorological Agency (JMA: accessed on 28 January 2021, [https://www.data.jma.go.jp/gmd/env/uvhp/info\\_uv.html](https://www.data.jma.go.jp/gmd/env/uvhp/info_uv.html)). According to the method of the JMA, the erythemal UV intensity ( $\text{mW}/\text{m}^2$ ) was calculated by multiplying the UVI by 25 times. Data on the near-surface chlorophyll concentration ( $\text{mg}/\text{m}^3$ ) were obtained from NASA's Ocean Color WEB (accessed on 15 December 2020 <https://oceancolor.gsfc.nasa.gov>). All data were recorded in 2020.

### 2.8. Statistical Analysis

Data are expressed as the mean  $\pm$  standard error. All values are the means of triplicate analysis. Statistical analysis was carried out using Tukey–Kramer's multiple comparisons test. All statistical analyses were performed using Statcel 3 software (version 3, OMS Publisher, Tokorozawa, Japan).

## 3. Results

### 3.1. Monthly Variation of Usujiri Dulce MAAs in 2020

We previously determined the extraction condition of MAAs from dulce [22]. In addition, the sampling period affected the MAA contents, with samples from late February to early April found to be suitable MAA sources in 2019. To confirm the sampling periods in 2020, we prepared crude MAAs and determined the quantities of MAAs from January to May in 2020. First, we confirmed the MAA components in 2020 by HPLC (Figure 1). The chromatogram showed six peaks (peaks a–f: shinorine, palythine, asterina-330, porphyra-334, usujirene, and palythene, respectively), which corresponded to the sample in 2019. We then determined the quantity of each MAA by HPLC (Table 1). The quantities of MAAs in 1 g of dry-weight dulce increased from January to March and decreased in April and May 2020. The 18 March sample showed the highest MAA content ( $6.696 \mu\text{mol}/\text{g}$  dry weight), while that of 27 May was the lowest ( $1.041 \mu\text{mol}/\text{g}$  dry weight).

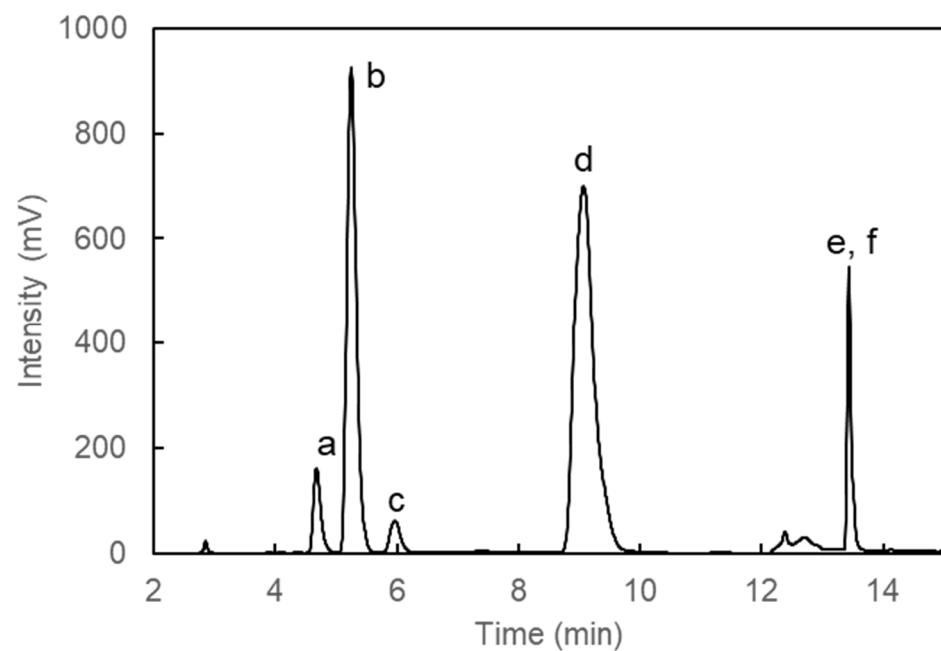


**Figure 1.** High Performance Liquid Chromatography (HPLC) chromatogram of crude dulse mycosporine-like amino acids (MAA) solution on 14 January 2020. MAAs were eluted by a linear gradient of acetonitrile from 0% at 7 min to 70% at 20 min. The data represent the typical peaks at retention times of 4.68 min (**a**, shinorine), 5.25 min (**b**, palythine), 5.97 min (**c**, asterina-330), 9.08 min (**d**, porphyra-334), and 13.44 min (**e**, usujirene, and **f**, palythene).

**Table 1.** MAA content in Usujiri dulse.

MAAs	Collection Date (2020)				
	14 January	13 February	18 March	27 April	27 May
Shinorine	0.167 ± 0.002 <sup>c</sup>	0.226 ± 0.001 <sup>a</sup>	0.215 ± 0.001 <sup>b</sup>	0.079 ± 0.003 <sup>d</sup>	0.031 ± 0.001 <sup>e</sup>
Palythine	2.444 ± 0.021 <sup>b</sup>	2.367 ± 0.019 <sup>b</sup>	2.625 ± 0.006 <sup>a</sup>	0.588 ± 0.019 <sup>c</sup>	0.493 ± 0.019 <sup>d</sup>
Asterina-330	0.080 ± 0.001 <sup>c</sup>	0.098 ± 0.001 <sup>b</sup>	0.108 ± 0.001 <sup>a</sup>	0.039 ± 0.001 <sup>d</sup>	0.019 ± 0.001 <sup>e</sup>
Porphyra-334	1.795 ± 0.015 <sup>c</sup>	1.940 ± 0.019 <sup>b</sup>	2.526 ± 0.024 <sup>a</sup>	0.640 ± 0.021 <sup>d</sup>	0.311 ± 0.015 <sup>e</sup>
Usujirene + Palythene	0.402 ± 0.003 <sup>c</sup>	0.750 ± 0.006 <sup>b</sup>	1.203 ± 0.006 <sup>a</sup>	0.623 ± 0.014 <sup>d</sup>	0.187 ± 0.008 <sup>e</sup>
Total	4.888 ± 0.035 <sup>c</sup>	5.380 ± 0.043 <sup>b</sup>	6.696 ± 0.002 <sup>a</sup>	1.968 ± 0.057 <sup>d</sup>	1.041 ± 0.044 <sup>e</sup>

MAA content is expressed as  $\mu\text{mol/g}$  dry weight. Data show mean values  $\pm$  SE,  $n = 3$ . Different letters for each MAA indicate significant differences in mean value (Tukey–Kramer’s multiple comparisons test,  $a\text{--}e < 0.05$ ).

### 3.2. Monthly Variation of MAA Contents

The molar percentage (mol%) contents in each MAA in 2020 were compared (Figure 2). The mol% values of shinorine (from 3.2 mol% on 18 March to 4.2 mol% on 13 February) and asterina-330 (from 1.6 mol% on 18 March to 2.0 mol% on 13 February) were stable at low values similar to the samples in 2019. The mol% of palythine decreased from 14 January (50 mol%) to 27 April (30 mol%), and then increased to 47 mol% on 27 May. Porphyra-334 was stable at approximately 37 mol% from 14 January to 18 May, and then gradually decreased to 30 mol% on 18 May. On the other hand, usujirene + palythene had a low mol% on 14 January (8.2 mol%), which increased up to 32 mol% on 27 April and then dropped to 18 mol% on 18 May. Among the five MAAs, the mol% of usujirene + palythene varied most greatly, ranging four-fold from 8.2 to 32 mol%, in a similar change to that observed in the dulse sample of 2019.

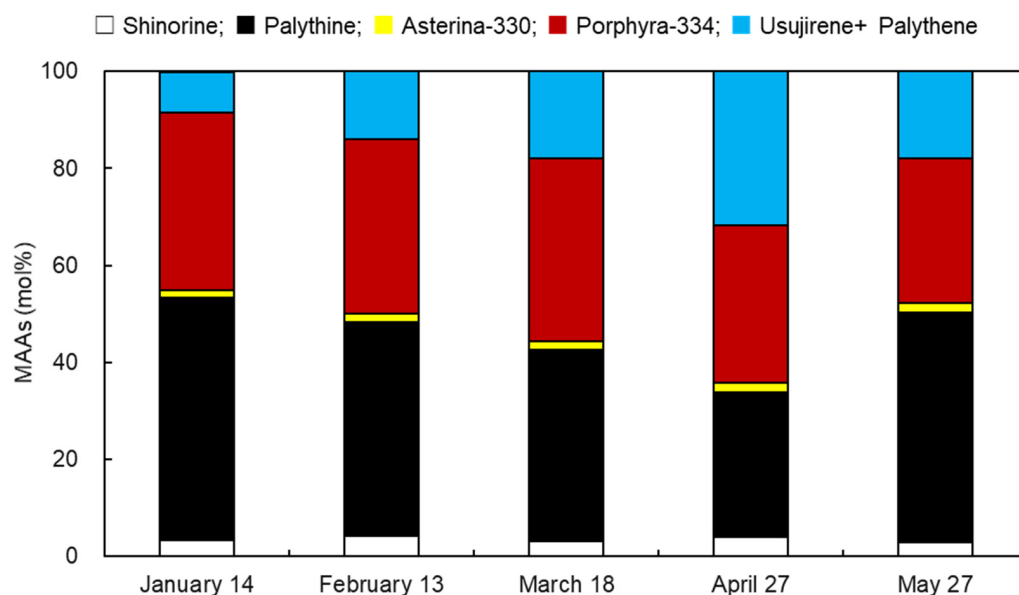


**Figure 2.** Molar percentages of MAAs in 2020. The quantities of six MAAs—shinorine, palythine, asterina-330, porphyra-334, and usujirene + palythene—were compared in dulse collected on 14 January, 13 February, 18 March, 27 April, and 27 May. The data show mean values,  $n = 3$ .

### 3.3. Change of MAAs, PE and Erythemat UV Intensity

To understand the variation of MAA content, data on the PE content and erythemat UV intensity were prepared (Figure 3). The PE contents were stable at 46  $\mu\text{g}/\text{mg}$  dry weight on 14 January and 13 February, and then gradually decreased from 13 February (47  $\mu\text{g}/\text{mg}$  dry weight) to 27 May (19  $\mu\text{g}/\text{mg}$  dry weight). Meanwhile, the erythemat UV intensity increased from January (25  $\text{mW}/\text{m}^2$ ) to May (115  $\text{mW}/\text{m}^2$ ). The total MAAs content correlated with the erythemat UV intensity from January to March, but it did not correlate with the PE content or erythemat UV intensity from April to May.

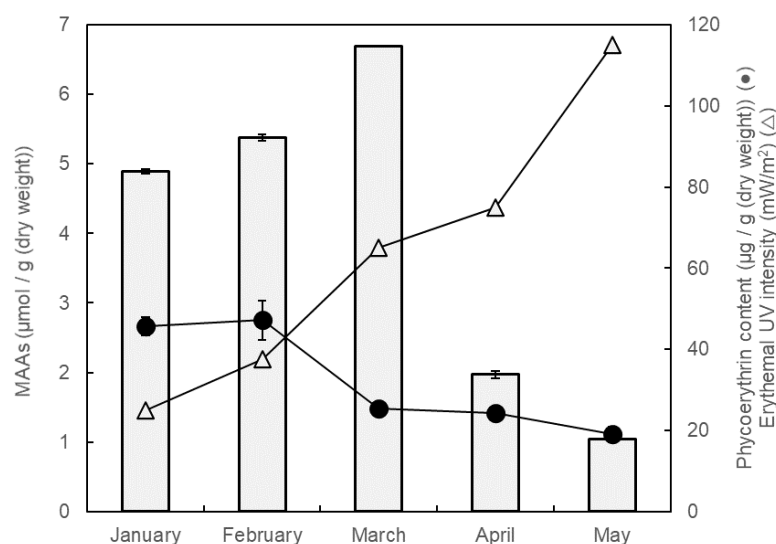


**Figure 3.** Monthly variation of MAAs and PE from dulse in 2020. The MAA quantity reflects the total of all MAAs. The quantity of PE from the dry weight was determined using the Beer and Eshel equation [36]. Erythemat UV intensity was obtained from the Japan Meteorological Agency.

### 3.4. Stability of Ultraviolet

One of the main functions of MAAs is absorption of UV radiation. Although studies on porphyra-334 and shinorine have been reported [31,37–39], there are few on palythine. We

prepared palythine and porphyra-334 and evaluated their UV stability. The strength of the UV radiation was set to  $200 \mu\text{W cm}^{-2}$ . We used 2-hydroxy-4-methoxybenzophenone and 2-ethylhexyl-4-methoxycinnamate as the non-sensitive and sensitive agent, respectively. The spectra of the two MAAs, palythine and porphyra-334, and 2-hydroxy-4-methoxybenzophenone were stable (Figure 4). However, 2-ethylhexyl-4-methoxycinnamate immediately changed from the trans-form to cis/trans-mixture forms [40]. This result showed that MAAs are stable UV-absorption-compounds.

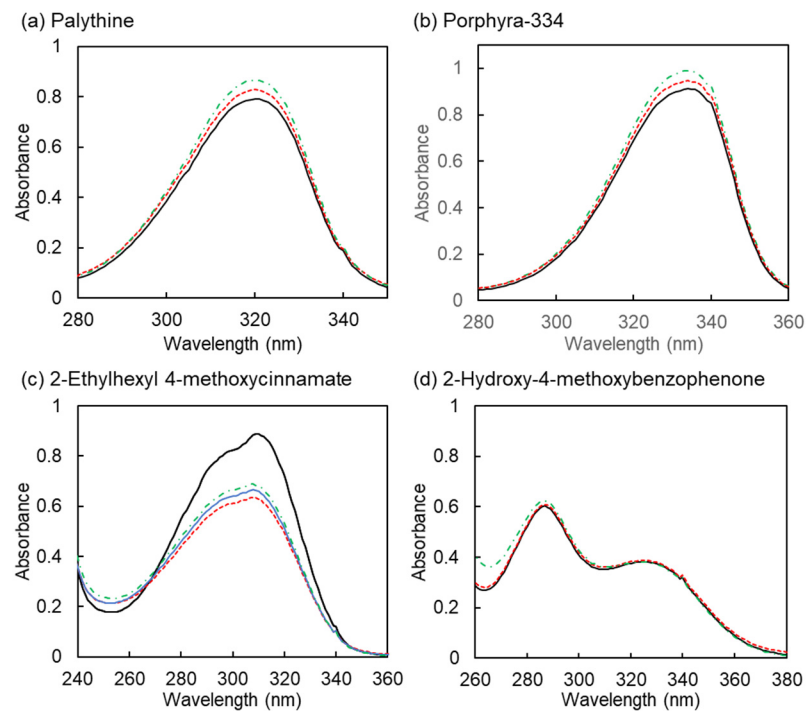


**Figure 4.** Spectra of UV-B exposure samples. Palythine and porphyra-334 were dissolved in 0.1 M sodium phosphate buffer (pH 7.4) at the concentration of  $2.2 \times 10^{-5}$  M. In the experiment, 2-hydroxy-4-methoxybenzophenone was dissolved in ethanol at the concentration of  $2.4 \times 10^{-5}$  M, while 2-ethylhexyl-4-methoxycinnamate was diluted with ethanol at the concentration of  $3.3 \times 10^{-6}$  M. UV-B (312 nm) was set at the radiation of  $200 \mu\text{W}/\text{cm}^2$ , and the spectra of samples were measured by a spectrophotometer. Black lines, 0 h; blue line, 1 h; red dotted lines, 6 h; green dashed lines, 12 h.

#### 4. Discussion

Our previous study showed that dulse from late February to early April in 2019 was suitable for MAA preparation [22] since dulse then disappeared in summer and reappeared in winter. To confirm the period, here, we investigated the suitable period of MAA preparation from dulse samples in 2020. The maximum quantities of MAAs in 2019 and 2020 were almost equal at  $6.930 \mu\text{mol/g}$  dry weight on 25 February 2019 and  $6.696 \mu\text{mol/g}$  dry weight on 18 March 2020 (Figure 5). Among the samples from January to May 2020, the MAA content was high in the samples from February to mid-March. The accumulation and loss of MAAs in 2020 differed from that of the 2019 samples. Specifically, the total MAAs on 14 January 2020 ( $4.888 \mu\text{mol/g}$ ) were higher than on 23 January 2019 ( $2.649 \mu\text{mol/g}$ ) [22]. The loss of MAAs on 27 April 2020 ( $1.968 \mu\text{mol/g}$ ) was faster than that on 17 May 2019 ( $4.972 \mu\text{mol/g}$ ). The difference between 2020 and 2019 was due to the quantity of palythine. In 2019 samples, this increased from January ( $1.739 \mu\text{mol/g}$ ) to May ( $3.255 \mu\text{mol/g}$ ); however, in 2020, it was stable from January ( $2.444 \mu\text{mol/g}$ ) to March ( $2.625 \mu\text{mol/g}$ ), and then drastically decreased in April ( $0.588 \mu\text{mol/g}$ ).

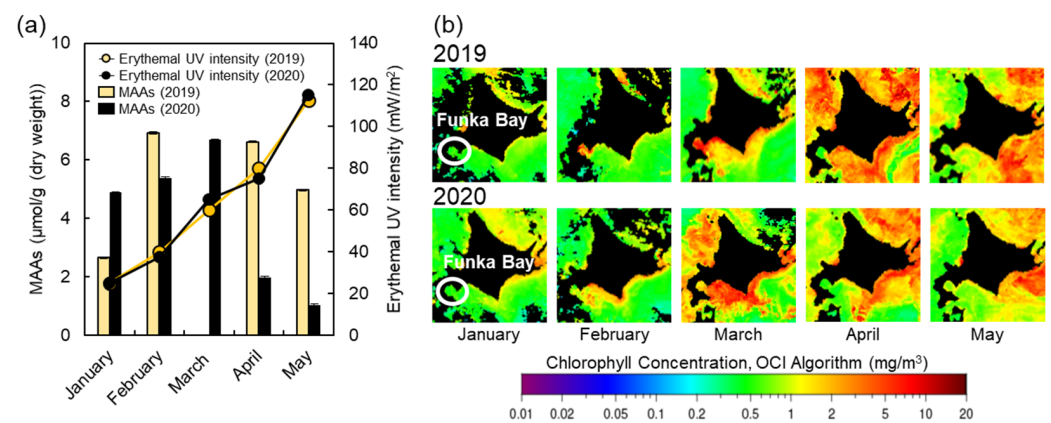


**Figure 5.** Monthly mean of MAA content, daily maximum erythemal UV intensity, and chlorophyll concentration in 2019 and 2020. (a) MAA content and erythemal UV intensity. Orange bar and line show MAA content and erythemal UV intensity in 2019; black bar and line show MAA content and erythemal UV intensity in 2020. (b) Chlorophyll concentration. These data were obtained from JMA and NASA's Ocean Color WEB. All data were recorded in 2019 and 2020.

We previously concluded that the decrease of MAAs was related to the increase of chlorophyll concentration around the Usujiri area, leading to a shortage of nitrogen sources for phytoplankton production. Although the quantities of total MAAs decreased in May 2020 versus 2019, the difference of palythine content may have occurred independently of the phytoplankton production. In this study, we employed the parameters of PE content, erythemal UV intensity, and chlorophyll concentration (data not shown: data from NASA's Ocean Color WEB). The PE content is one of the factors reflecting the quantity of nitrogen compounds in red algae [41–43], suggesting that the loss of PE in dulse was due to a reduction of nitrogen compounds in the sea, along with the increase in the chlorophyll concentration in the Usujiri area. Erythemal UV intensity increases the quantity of MAAs in seaweeds [44], which present as nitrogen compounds in seaweeds. The decrease of MAAs from March to April was slow compared to that of PE from February to March, indicating that MAAs are essential compounds in red algae. However, the MAA contents did not increase with erythemal UV intensity. To understand each MAA's content involves taking account of the many reasons for MAAs' accumulation such as nutrients, stress from water temperature, and desiccation [45–48]. From these two-year results, we propose that a suitable sampling period for Usujiri dulse for MAA preparation extends from mid-February to early April.

Although MAAs were unstable in conditions that were acidic (lower than pH 3.0) or alkaline (higher than pH 10.5), as well as at hot temperatures (higher than 60 °C) [10], MAAs were stable at moderate conditions of pH 4.0 to 8.5 and temperatures up to 50 °C [10]. Reports on the UV stability of MAAs are rare. We demonstrated the UV stability of MAAs for up to 12 h in the expected conditions in the summer season of Wellington, New Zealand, which is one of the most high-strength locations of radiation on Earth. The MAAs in this study released heat from UV radiation and were unstable above 60 °C, but we propose that the experimental conditions (UV irradiation and MAA concentration) represent a tolerant range of heating for the sample solvent.

Not only do marine photosynthetic organisms use MAAs for UV protection, but also non-MAA producers such as fish and invertebrates incorporate and use MAAs for UV protection [25,26,49,50]. Many UV protection agents in products are lipid-soluble materials. MAAs are the amphiphilic compounds. These results show that MAAs have the potential for use as natural UV protection compounds.

## 5. Conclusions

We clarified the seasonal variation of Usujiri dulse MAA contents in 2020. Comparing these with the MAA variation in 2019, we conclude that MAA preparation of samples

from Usujiri dulse may be carried out from mid-February to early April. However, the composition of MAAs differed between the two years. We, therefore, need to investigate MAAs' contents in the long term. In addition, we showed the UV stability of MAAs under pH-controlled conditions. This information will be helpful for the application of MAAs to produce eco-friendly materials.

**Author Contributions:** H.K. and Y.K. conceived and designed the research; Y.N. performed the experiments; Y.N. and Y.M. analyzed the data; Y.K. and H.K. contributed to writing and editing the manuscript. All authors have read and agreed to the published version of the manuscript.

**Funding:** This research received no external funding.

**Institutional Review Board Statement:** Not applicable.

**Informed Consent Statement:** Not applicable.

**Data Availability Statement:** The data is contained within the article.

**Acknowledgments:** We gratefully acknowledge sampling assistance with *Palmaria palmata* in Japan at Usujiri from Hiroyuki Munehara, Atsuya Miyajima and Chikara Kawagoe. We also acknowledge research assistance with MAA preparation from Kanami Sugiyama.

**Conflicts of Interest:** The authors declare no conflict of interest.

## References

1. Zhang, X.; Rosenstein, B.S.; Wang, Y.; Lebowitz, M.; Wei, H. Identification of Possible Reactive Oxygen Species Involved in Ultraviolet Radiation-Induced Oxidative DNA Damage. *Free Radic. Biol. Med.* **1997**, *23*, 980–985. [[CrossRef](#)]
2. Pillai, S.; Oresajo, C.; Hayward, J. Ultraviolet radiation and skin aging: Roles of reactive oxygen species, inflammation and protease activation, and strategies for prevention of inflammation-induced matrix degradation—A review. *Int. J. Cosmet. Sci.* **2005**, *27*, 17–34. [[CrossRef](#)] [[PubMed](#)]
3. Neale, R.E.; Khan, S.R.; Lucas, R.M.; Waterhouse, M.; Whiteman, D.C.; Olsen, C.M. The effect of sunscreen on vitamin D: A review. *Br. J. Dermatol.* **2019**, *181*, 907–915. [[CrossRef](#)] [[PubMed](#)]
4. Danno, K.; Horio, T.; Imamura, S. Infrared radiation suppresses ultraviolet B-induced sunburn-cell formation. *Arch. Dermatol. Res.* **1992**, *284*, 92–94. [[CrossRef](#)]
5. Matsumura, Y.; Ananthaswamy, H.N. Short-term and long-term cellular and molecular events following UV irradiation of skin: Implications for molecular medicine. *Expert Rev. Mol. Med.* **2002**, *4*, 1–22. [[CrossRef](#)] [[PubMed](#)]
6. Young, A.R. Acute effects of UVR on human eyes and skin. *Prog. Biophys. Mol. Biol.* **2006**, *92*, 80–85. [[CrossRef](#)]
7. Ma, H.; Brennan, A.; Diamond, S.A. Photocatalytic reactive oxygen species production and phototoxicity of titanium dioxide nanoparticles are dependent on the solar ultraviolet radiation spectrum. *Environ. Toxicol. Chem.* **2012**, *31*, 2099–2107. [[CrossRef](#)]
8. Schauder, S.; Ippen, H. Contact and photocontact sensitivity to sunscreens. *Contact Dermat.* **1997**, *37*, 221–232. [[CrossRef](#)]
9. Greenspoon, J.; Ahluwalia, R.; Juma, N.; Rosen, C.F. Allergic and Photoallergic Contact Dermatitis: A 10-year Experience. *Dermatitis* **2013**, *24*, 29–32. [[CrossRef](#)]
10. de la Coba, F.; Aguilera, J.; Korbee, N.; de Gálvez, M.V.; Herrera-Ceballos, E.; Álvarez-Gómez, F.; Figueroa, F.L. UVA and UVB Photoprotective Capabilities of Topical Formulations Containing Mycosporine-like Amino Acids (MAAs) through Different Biological Effective Protection Factors (BEPFs). *Mar. Drugs* **2019**, *17*, 55. [[CrossRef](#)]
11. Danovaro, R.; Bongiorni, L.; Corinaldesi, C.; Giovannelli, D.; Damiani, E.; Astolfi, P.; Greci, L.; Pusceddu, A. Sunscreens Cause Coral Bleaching by Promoting Viral Infections. *Environ. Health Perspect.* **2008**, *116*, 441–447. [[CrossRef](#)] [[PubMed](#)]
12. Rancan, F.; Rosan, S.; Boehm, K.; Fernández, E.; Hidalgo, M.E.; Quihot, W.; Rubio, C.; Boehm, F.; Piazena, H.; Oltmanns, U. Protection against UVB irradiation by natural filters extracted from lichens. *J. Photochem. Photobiol. B Biol.* **2002**, *68*, 133–139. [[CrossRef](#)]
13. Nobile, V.; Michelotti, A.; Cestone, E.; Caturla, N.; Castillo, J.; Benavente-García, O.; Pérez-Sánchez, A.; Micol, V. Skin photoprotective and antiageing effects of a combination of rosemary (*Rosmarinus officinalis*) and grapefruit (*Citrus paradisi*) polyphenols. *Food Nutr. Res.* **2016**, *60*, 31871. [[CrossRef](#)] [[PubMed](#)]
14. Pérez-Sánchez, A.; Barrajón-Catalán, E.; Caturla, N.; Castillo, J.; Benavente-García, O.; Alcaraz, M.; Micol, V. Protective effects of citrus and rosemary extracts on UV-induced damage in skin cell model and human volunteers. *J. Photochem. Photobiol. B Biol.* **2014**, *136*, 12–18. [[CrossRef](#)] [[PubMed](#)]
15. Furuta, T.; Miyabe, Y.; Yasui, H.; Kinoshita, Y.; Kishimura, H. Angiotensin I converting enzyme inhibitory peptides derived from phycobiliproteins of dulse *Palmaria palmata*. *Mar. Drugs* **2016**, *14*, 32. [[CrossRef](#)] [[PubMed](#)]
16. Sato, N.; Furuta, T.; Takeda, T.; Miyabe, Y.; Ura, K.; Takagi, Y.; Yasui, H.; Kumagai, Y.; Kishimura, H. Antioxidant activity of proteins extracted from red alga dulse harvested in Japan. *J. Food Biochem.* **2019**, *43*, e12709. [[CrossRef](#)] [[PubMed](#)]

17. Yamamoto, Y.; Kishimura, H.; Kinoshita, Y.; Saburi, W.; Kumagai, Y.; Yasui, H.; Ojima, T. Enzymatic production of xylooligosaccharides from red alga dulse (*Palmaria* sp.) wasted in Japan. *Process Biochem.* **2019**, *82*, 117–122. [[CrossRef](#)]
18. Kobayashi, M.; Kumagai, Y.; Yamamoto, Y.; Yasui, H.; Kishimura, H. Identification of a Key Enzyme for the Hydrolysis of  $\beta$ -(1→3)-Xylosyl Linkage in Red Alga Dulse Xylooligosaccharide from *Bifidobacterium Adolescentis*. *Mar. Drugs* **2020**, *18*, 174. [[CrossRef](#)]
19. Miyabe, Y.; Furuta, T.; Takeda, T.; Kanno, G.; Shimizu, T.; Tanaka, Y.; Gai, Z.; Yasui, H.; Kishimura, H. Structural Properties of Phycoerythrin from Dulse *Palmaria palmata*. *J. Food Biochem.* **2017**, *4*, 12301. [[CrossRef](#)]
20. Kumagai, Y.; Tsubouchi, R.; Miyabe, Y.; Takeda, T.; Adachi, K.; Yasui, H.; Kishimura, H. Complete sequence of mitochondrial DNA of red alga dulse *Palmaria palmata* (Linnaeus) Weber & Mohr in Japan. *Mitochondrial DNA Part B* **2019**, *4*, 3177–3178.
21. Kumagai, Y.; Miyabe, Y.; Takeda, T.; Adachi, K.; Yasui, H.; Kishimura, H. In Silico Analysis of Relationship between Proteins from Plastid Genome of Red Alga *Palmaria* sp. (Japan) and Angiotensin I Converting Enzyme Inhibitory Peptides. *Mar. Drugs* **2019**, *17*, 190. [[CrossRef](#)]
22. Nishida, Y.; Kumagai, Y.; Michiba, S.; Yasui, H.; Kishimura, H. Efficient Extraction and Antioxidant Capacity of Mycosporine-Like Amino Acids from Red Alga Dulse *Palmaria palmata* in Japan. *Mar. Drugs* **2020**, *18*, 502. [[CrossRef](#)] [[PubMed](#)]
23. Balskus, E.P.; Walsh, C.T. The Genetic and Molecular Basis for Sunscreen Biosynthesis in Cyanobacteria. *Science* **2010**, *329*, 1653–1656. [[CrossRef](#)] [[PubMed](#)]
24. Shick, J.M.; Dunlap, W.C. Mycosporine-Like Amino Acids and Related Gadusols: Biosynthesis, Accumulation, and UV-Protective Functions in Aquatic Organisms. *Annu. Rev. Physiol.* **2002**, *64*, 223–262. [[CrossRef](#)] [[PubMed](#)]
25. Karentz, D.; McEuen, F.S.; Land, M.C.; Dunlap, W.C. Survey of mycosporine-like amino acid compounds in Antarctic marine organisms: Potential protection from ultraviolet exposure. *Mar. Biol.* **1991**, *108*, 157–166. [[CrossRef](#)]
26. Banaszak, A.T.; Trench, R.K. Effects of ultraviolet (UV) radiation on marine microalgal-invertebrate symbioses. II. The synthesis of mycosporine-like amino acids in response to exposure to UV in *Anthopleura elegantissima* and *Cassiopeia xamachana*. *J. Exp. Mar. Biol. Ecol.* **1995**, *194*, 233–250. [[CrossRef](#)]
27. Chrapusta, E.; Kaminski, A.; Zabaglo, K.; Bober, B.; Adamski, M.; Bialczyk, J. Mycosporine-like amino acids: Potential health and beauty ingredients. *Mar. Drugs* **2017**, *15*, 326. [[CrossRef](#)] [[PubMed](#)]
28. Karsten, U.; Sawall, T.; Wiencke, C. A survey of the distribution of UV-absorbing substances in tropical macroalgae. *Phycol. Res.* **1998**, *46*, 271–279.
29. Chuang, L.F.; Chou, H.N.; Sung, P.J. Porphyra-334 isolated from the marine algae *Bangia atropurpurea*: Conformational performance for energy conversion. *Mar. Drugs* **2014**, *12*, 4732–4740. [[CrossRef](#)]
30. Conde, F.R.; Carignan, M.O.; Churio, M.S.; Carreto, J.I. In Vitro cis–trans photoisomerization of palythene and usujirene. Implications on the *in vivo* transformation of mycosporine-like amino acids. *Photochem. Photobiol.* **2003**, *77*, 146–150. [[CrossRef](#)]
31. Conde, F.R.; Churio, M.S.; Previtali, C.M. The photoprotector mechanism of mycosporine-like amino acids. Excited-state properties and photostability of porphyra-334 in aqueous solution. *J. Photochem. Photobiol. B Biol.* **2000**, *56*, 139–144. [[CrossRef](#)]
32. Torres, P.; Santos, J.; Chow, F.; Ferreira, M.J.P.; Santos, D. Comparative analysis of in vitro antioxidant capacities of mycosporine-like amino acids (MAAs). *Algal Res.* **2018**, *34*, 57–67. [[CrossRef](#)]
33. Whittock, A.L.; Auckloo, N.; Cowden, A.M.; Turner, M.A.P.; Woolley, J.M.; Wills, M.; Corre, C.; Stavros, V.G. Exploring the blueprint of photoprotection in mycosporine-like amino acids. *J. Phys. Chem. Lett.* **2021**, *12*, 3641–3646. [[CrossRef](#)]
34. Diehl, N.; Michalik, D.; Zuccarello, G.C.; Karsten, U. Stress metabolite pattern in the eulittoral red alga *Pyropia plicata* (Bangiales) in New Zealand—Mycosporine-like amino acids and heterosides. *J. Exp. Mar. Biol. Ecol.* **2019**, *510*, 23–30. [[CrossRef](#)]
35. Jofre, J.; Celis-Plá, P.S.M.; Figueroa, F.L.; Navarro, N. Seasonal variation of mycosporine-like amino acids in three subantarctic red seaweeds. *Mar. Drugs* **2020**, *18*, 75. [[CrossRef](#)]
36. Beer, S.; Eshel, A. Determining phycoerythrin and phycocyanin concentrations in aqueous crude extracts of red algae. *Mar. Freshw. Res.* **1985**, *36*, 785–792. [[CrossRef](#)]
37. Karsten, U.; Franklin, L.A.; Lüning, K.; Wiencke, C. Natural ultraviolet radiation and photosynthetically active radiation induce formation of mycosporine-like amino acids in the marine macroalga *Chondrus crispus* (Rhodophyta). *Planta* **1998**, *205*, 257–262. [[CrossRef](#)]
38. Bhatia, S.; Sharma, K.; Namdeo, A.G.; Chaugule, B.B.; Kavale, M.; Nanda, S. Broad-spectrum sun-protective action of Porphyra-334 derived from *Porphyra vietnamensis*. *Pharmacogn. Res.* **2010**, *2*, 45–49. [[CrossRef](#)]
39. Rastogi, R.P.; Incharoensakdi, A. UV radiation-induced biosynthesis, stability and antioxidant activity of mycosporine-like amino acids (MAAs) in a unicellular cyanobacterium *Gloeocapsa* sp. CU2556. *J. Photochem. Photobiol. B Biol.* **2014**, *130*, 287–292. [[CrossRef](#)]
40. Herzog, B.; Amorós-Galicia, L.; Sohn, M.; Hofer, M.; Quass, K.; Giesinger, J. Analysis of photokinetics of 2'-ethylhexyl-4-methoxycinnamate in sunscreens. *Photochem. Photobiol. Sci.* **2019**, *18*, 1773–1781. [[CrossRef](#)]
41. Dupré, C.; Guary, J.-C.; Grizeau, D. Effect of photon fluence rate, nitrogen limitation and nitrogen recovery on the level of phycoerythrin in the unicellular alga, *Rhodorus marinus* (Rhodophyceae). *Physiol. Plant.* **1994**, *92*, 521–527. [[CrossRef](#)]
42. Hsieh-Lo, M.; Castillo, G.; Ochoa-Becerra, M.A.; Mojica, L. Phycocyanin and phycoerythrin: Strategies to improve production yield and chemical stability. *Algal Res.* **2019**, *42*, 521–527. [[CrossRef](#)]
43. Sosa-Hernández, J.E.; Rodas-Zuluaga, L.I.; Castillo-Zacarías, C.; Rostro-Alanís, M.; de la Cruz, R.; Carrillo-Nieves, D.; Salinas-Salazar, C.; Fuentes Grunewald, C.; Llewellyn, C.A.; Olguín, E.J.; et al. Light intensity and nitrogen concentration impact on the biomass and phycoerythrin production by *Porphyridium purpureum*. *Mar. Drugs* **2019**, *17*, 460. [[CrossRef](#)]

44. Hoyer, K.; Karsten, U.; Sawall, T.; Wiencke, C. Photoprotective substances in Antarctic macroalgae and their variation with respect to depth distribution, different tissues and developmental stages. *Mar. Ecol. Prog. Ser.* **2001**, *211*, 117–129. [[CrossRef](#)]
45. Korbee, N.; Huovinen, P.; Figueroa, F.L.; Aguilera, J.; Karsten, U. Availability of ammonium influences photosynthesis and the accumulation of mycosporine-like amino acids in two *Porphyra* species (Bangiales, Rhodophyta). *Mar. Biol.* **2005**, *146*, 645–654. [[CrossRef](#)]
46. Jiang, H.; Gao, K.; Helbling, E.W. UV-absorbing compounds in *Porphyra haitanensis* (Rhodophyta) with special reference to effects of desiccation. *Environ. Boil. Fishes* **2007**, *20*, 387–395. [[CrossRef](#)]
47. Carreto, J.I.; Carignan, M.O. Mycosporine-like amino acids: Relevant secondary metabolites. Chemical and ecological aspects. *Mar. Drugs* **2011**, *9*, 387–446. [[CrossRef](#)]
48. Briani, B.; Sissini, M.N.; Lucena, L.A.; Batista, M.B.; Costa, I.O.; Nunes, J.M.C.; Schmitz, C.; Ramlov, F.; Maraschin, M.; Korbee, N.; et al. The influence of environmental features in the content of mycosporine-like amino acids in red marine algae along the Brazilian coast. *J. Phycol.* **2018**, *54*, 380–390. [[CrossRef](#)] [[PubMed](#)]
49. Mason, D.S.; Schafer, F.; Shick, J.M.; Dunlap, W.C. Ultraviolet radiation-absorbing mycosporine-like amino acids (MAAs) are acquired from their diet by medaka fish (*Oryzias latipes*) but not by SKH-1 hairless mice. *Comp. Biochem. Physiol. Part A Mol. Integr. Physiol.* **1998**, *120*, 587–598. [[CrossRef](#)]
50. Hartmann, A.; Holzinger, A.; Ganzera, M.; Karsten, U. Prasiolin, a new UV-sunscreen compound in the terrestrial green macroalga *Prasiola calophylla* (Carmichael ex Greville) Kützinger (Trebouxiophyceae, Chlorophyta). *Planta* **2016**, *243*, 161–169. [[CrossRef](#)] [[PubMed](#)]